

# Identification of Parameters of a Nonlinear Material Model Considering the Effects of Viscoelasticity and Damage

J. Heczko<sup>1</sup>, R. Kottner<sup>2</sup>, and T. Kroupa<sup>2</sup>

**Abstract:** This work deals with mechanical properties of a rubber material that is used in modern tram wheels as a damping element. Nonlinear static response as well as strain softening and hysteresis are captured in the material model. The identification method of the model's parameters is developed. The identification method relies on successive minimizations with respect to different sets of parameters. The identification of the parameters of the material model is based on the tensile and compressive experimental data. Shear data are used for validation.

**Keywords:** Rubber, hyperelasticity, viscoelasticity, Mullins effect

## 1 Introduction

Elastomeric materials are nowadays an inherent part of many structures thanks to their good vibration damping properties and ability to reach large deformations without a failure. An example of an elastomeric part is the utilization of rubber segments in modern tram wheels. These rubber sprung wheels excel in reduction of traffic noise and rail wear. Innovation of the wheels requires sufficient computational model of the rubber segments that considers the segment's complex mechanical behavior. Besides nonlinear response, the most noticeable phenomena observable in mechanical behavior of elastomers are: strain induced softening (Mullins effect, Mullins (1969)), hysteresis (Bergström and Boyce (1998)), and permanent set (Amin, Lion, Sekita, and Okui (2006)).

Objectives of this article were: (i) Select a constitutive model that is able to capture the effects of nonlinear long-term response, strain induced softening and time-dependence in mechanical behavior of a material. (ii) Develop a method to identify

---

<sup>1</sup> Department of Mechanics, Faculty of Applied Sciences, University of West Bohemia

<sup>2</sup> European Centre of Excellence, New Technologies for Information Society, Faculty of Applied Sciences, University of West Bohemia

parameters of the model. (iii) Apply the method to the rubber of the wheel segments.

## 2 Material model

### 2.1 Strain induced softening

Mullins effect was captured using the Ogden-Roxburgh model (proposed in Ogden and Roxburgh (1999)) of strain induced softening. The model can be described as follows.

An internal variable  $\eta$  is introduced to quantify the damage at a given material point. The strain energy density function can be written as

$$W = W(\mathbf{F}, \eta) = W(\lambda_1, \lambda_2, \lambda_3, \eta) = \eta \cdot W(\lambda_1, \lambda_2, \lambda_3), \quad (1)$$

where  $\lambda_1$ ,  $\lambda_2$  and  $\lambda_3$  are the principal stretches.

As a suitable representation of the strain energy density function, the five-parameter Mooney-Rivlin model was chosen in this paper:

$$W_{MR}(\lambda_1, \lambda_2, \lambda_3) = C_{10}(I_1 - 3) + C_{01}(I_2 - 3) + C_{11}(I_1 - 3)(I_2 - 3) + C_{20}(I_1 - 3)^2 + C_{30}(I_1 - 3)^3, \quad (2)$$

where  $I_1 = \lambda_1^2 + \lambda_2^2 + \lambda_3^2$  and  $I_2 = \lambda_1^2\lambda_2^2 + \lambda_2^2\lambda_3^2 + \lambda_1^2\lambda_3^2$ .

The damage variable  $\eta$  in the Ogden-Roxburgh model is expressed as

$$\eta = 1 - \frac{1}{r} \operatorname{erf} \left( \frac{(W_m - W(\lambda_1, \lambda_2, \lambda_3))}{m - \beta W_m} \right), \quad (3)$$

where  $r$ ,  $m$  and  $\beta$  are parameters of the model,  $W_m$  is the maximum strain energy density achieved at the material point during the loading prior to the current time.

### 2.2 Finite-strain viscoelasticity

To introduce time dependency of the material behavior, the concept of free energy was used. The development of Simo (1987) for derivation of stress-strain relationships was used. The second Piola-Kirchhoff stress is

$$\mathbf{S} = \int_0^t K(t-s) \frac{d}{ds} \left( \eta(W_m) \frac{\partial W_{MR}}{\partial \mathbf{E}} \right) ds, \quad (4)$$

where  $K(t)$  is a relaxation function. Usually it is expressed in the form

$$K(t) = \delta_0 + \sum_{n=1}^N \delta_n e^{-t/\tau_n} \quad (5)$$

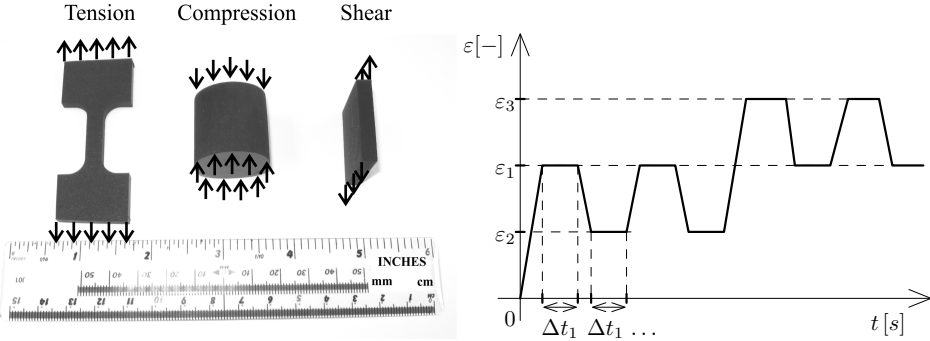


Figure 1: Experimental specimens (left), prescribed deformation (right).

which involves more values of relaxation times  $\tau_n$  and coefficients  $\delta_n$ , where the number of the viscoelastic terms,  $N$ , must be chosen according to the number of time scales that have to be modeled. Apart from the values of  $\delta_n$  and  $\tau_n$  all being positive, a natural requirement on the coefficients is that  $\delta_0 + \delta_1 + \dots + \delta_N = 1$ .

### 3 Experiments

The tram wheel segments are made from rubber based on synthetic isoprene and butadiene elastomers. Experimental samples had to be cut directly from the segments. The small size of the segments limited the specimens geometry, therefore all test method recommendations (Brown (2006)) could not be complied. Fig. 1 illustrates used shapes of the experimental specimens. Three types of tests were performed: the tension, the compression and the simple shear test.

Major deformations of the real wheel segments are compressive and the minor deformations are shear. Predominantly, the segment strain magnitude ranges from 10 to 15%. Maximum strain magnitude is 25%. Therefore, prescribed deformation progress during the experiments was as shown in Fig. 1. The strain rate was  $0.4 \text{ min}^{-1}$  in all performed tests. The results were obtained in room temperature of  $20^\circ\text{C}$  to  $25^\circ\text{C}$ .

### 4 Solution of the state problems

As shown in section 5, a boundary value problem (BVP) has to be defined for each experiment (tension, compression) in order to define the parameter identification problem. A state of uniform uniaxial strain can be assumed in the measured part of the tensile specimen. Therefore, the tensile test does not need to be simulated using the finite element method (FEM) because the true stress can be computed directly

from the experimental data. The strain distribution in a compression specimen is not uniform because it is not possible to fully avoid the friction between the specimen and the loading plates. The strain distribution in the shear specimen is also influenced, in this case, by adhesively bonded loading plates. Therefore, the compression and shear tests were simulated using FEM in Abaqus 6.11 software.

## 5 The identification problem

Let us consider a system the state of which at a time step  $t^{(i)}$  is described by a vector  $y^{(i)}$ . The measured quantity and its computed counterpart are denoted  $\bar{\varphi}_i$  and  $\varphi(\mathbf{x}, y^{(i)})$  respectively, where  $\mathbf{x}$  denotes the vector of material parameters.

As mentioned above, three experiments were performed in different modes of loading. The shear loading mode was not used in the identification because of significantly higher requirement on FEM computational time. The shear simulation response was used only for the validation of the identified parameters.

The tensile and compressive loading modes represent two different state problems and two different sets of measured data  $\bar{\varphi}_i$  that must together lead to a single set of material parameters  $\mathbf{x}$ . To account for this, the objective function

$$F(\mathbf{x}) = \frac{\sum_{i \in I} (\bar{\varphi}_i^t - \varphi^t(\mathbf{x}, y^{(i)}))^2}{\sum_{i \in I} (\bar{\varphi}_i^t)^2} + \frac{\sum_{i \in I} (\bar{\varphi}_i^c - \varphi^c(\mathbf{x}, y^{(i)}))^2}{\sum_{i \in I} (\bar{\varphi}_i^c)^2} \quad (6)$$

was minimized. The set  $I$  is a set of all time steps in which the quantity  $\bar{\varphi}_i$  was measured. The upper index  $t$  or  $c$  denotes value corresponding either to the tension or the compression experiment/model. The sums in denominators were introduced to compensate for the difference of magnitude of response in tension and compression. In this work, the response in tension was calculated analytically and the response in compression was the force computed by the finite element method.

Considering that in the Ogden-Roxburgh model (OR) the damage does not evolve when  $W_m = W$ , we can identify the Mooney-Rivlin (MR) hyperelastic parameters ( $C_{ij}$ ) first (considering only the first-loading parts of data). The parameters of the OR model ( $r, m, \beta$ ) can be identified independently afterwards, considering, similarly, only the reloading paths.

However, the identification of the viscoelastic parameters ( $\delta_n, \tau_n$ ) cannot be performed without adjusting at least the MR parameters because viscoelasticity affects the response of the material in every time step. This part of the identification has been divided into three steps. Firstly, MR and viscoelastic parameters are identified, the vector of variables  $\mathbf{x} = [c_{MR}; \delta_n, \tau_n]$ . The parameter  $c_{MR}$  serves for roughly adjusting the overall stiffness by multiplying the MR parameters that have

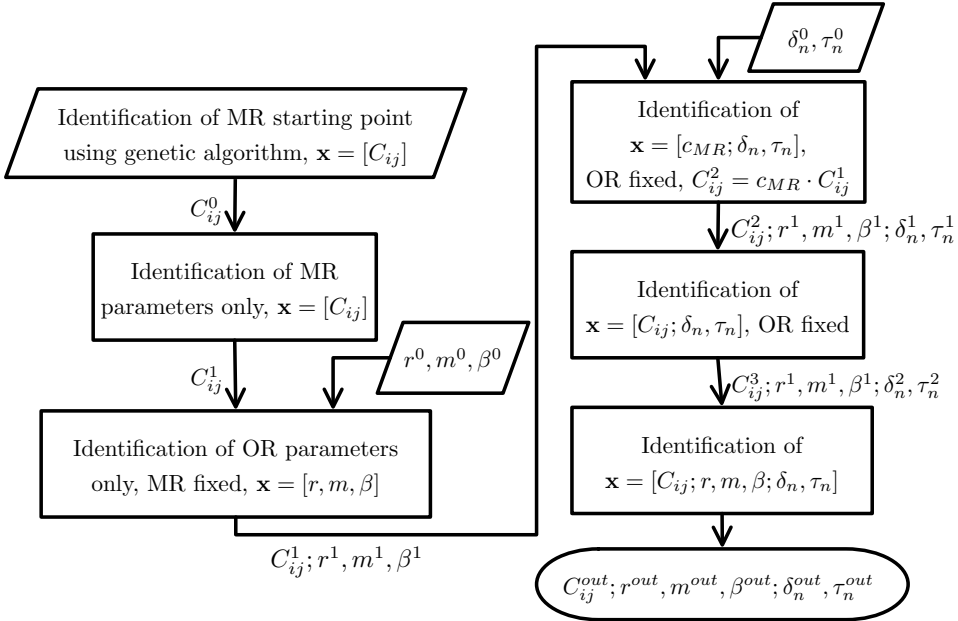


Figure 2: Block diagram of the identification process.

been identified earlier. Secondly, all MR parameters are treated as separate optimization variables in addition to the viscoelasticity parameters,  $\mathbf{x} = [C_{ij}; \delta_n, \tau_n]$ . Thirdly, all previous successive steps lead to the final optimization of all parameters,  $\mathbf{x} = [C_{ij}; r, m, \beta; \delta_n, \tau_n]$  (see Fig. 2).

The starting point for the identification of MR parameters was obtained by a genetic algorithm in OptiSLang software. All other minimizations were carried out using the interior-point algorithm that is part of the Matlab Optimization Toolbox.

## 6 Identification results

Using the procedure described in section 5, a set of model parameters was obtained. Fig. 3 shows the comparison of stress-strain curves of the model and experiment in tension and force-displacement curves for the case of compression. From the model response in compression and shear a significant increase of stiffness was obvious at strain values close to maximum. Therefore, maximum operational deformations have to be known prior to the identification to ensure that the investigated strain range is wider than the operational strain range. If there are any uncertainties about the operational strain range, the objective function should be adjusted to include final tangent of the model response.

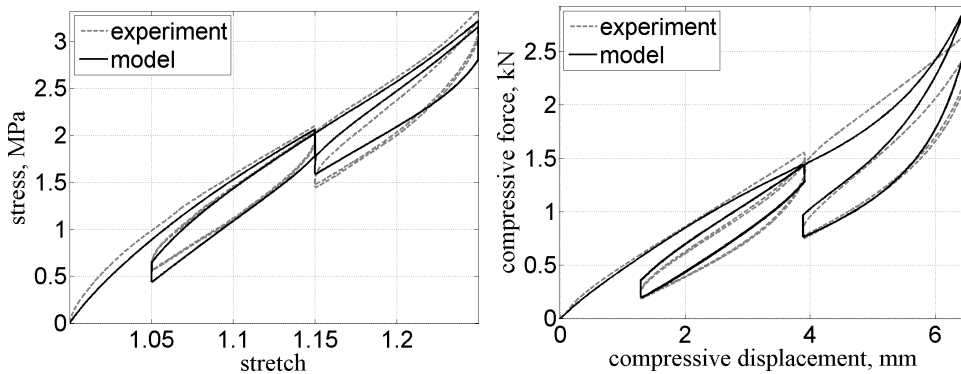


Figure 3: Stress-stretch curve of tensile test (left), force-displacement curve of compression test (right).

## 7 Conclusion

In this work, a material model capable of describing dominant mechanical properties of the analyzed rubber was composed. The rubber is used as a damping element in tram wheels. Applicable method of the identification of parameters of the material model was proposed. The comparison of numerical simulations and all experiments was in sufficient agreement although the simple shear test was not used directly in the identification process.

**Acknowledgement:** This work was supported by the European Regional Development Fund (ERDF), project NTIS - New Technologies for Information Society, European Centre of Excellence, CZ.1.05/1.1.00/02.0090.

## References

- Amin, A.; Lion, A.; Sekita, S.; Okui, Y.** (2006): Nonlinear dependence of viscosity in modeling the rate-dependent response of natural and high damping rubbers in compression and shear: Experimental identification and numerical verification. *International Journal of Plasticity*, vol. 22, pp. 1610–1657.
- Bergström, J.; Boyce, M.** (1998): Constitutive modeling of the large strain time-dependent behavior of elastomers. *Journal of the Mechanics and Physics of Solids*, vol. 46, no. 5, pp. 931–954.
- Brown, R.** (2006): *Physical Testing of Rubber*. Springer.
- Mullins, L.** (1969): Softening of rubber by deformation. *Rubber Chemistry and Technology*, vol. 42, no. 1, pp. 339–362.

**Ogden, R. W.; Roxburgh, D. G.** (1999): A pseudo-elastic model for the Mullins effect in filled rubber. *Proc. R. Soc. Lond. A*, , no. 455, pp. 2861–2877.

**Simo, J. C.** (1987): On a fully three-dimensional finite-strain viscoelastic damage model: Formulation and computational aspects. *Computer Methods in Applied Mechanics and Engineering*, vol. 60, pp. 153–173.

